

---

Masters Theses

Student Theses and Dissertations

---

1964

## A study of the crystallographic orientation dependence of electrical resistivity in zinc

Paul Frederic Becher

Follow this and additional works at: [https://scholarsmine.mst.edu/masters\\_theses](https://scholarsmine.mst.edu/masters_theses)



Part of the [Metallurgy Commons](#)

Department:

---

### Recommended Citation

Becher, Paul Frederic, "A study of the crystallographic orientation dependence of electrical resistivity in zinc" (1964). *Masters Theses*. 5676.

[https://scholarsmine.mst.edu/masters\\_theses/5676](https://scholarsmine.mst.edu/masters_theses/5676)

This thesis is brought to you by Scholars' Mine, a service of the Missouri S&T Library and Learning Resources. This work is protected by U. S. Copyright Law. Unauthorized use including reproduction for redistribution requires the permission of the copyright holder. For more information, please contact [scholarsmine@mst.edu](mailto:scholarsmine@mst.edu).

A STUDY OF THE CRYSTALLOGRAPHIC  
ORIENTATION DEPENDENCE OF ELECTRICAL  
RESISTIVITY IN ZINC

BY

Paul Fredric Becher, 1941

---

A

THESIS

submitted to the faculty of the

UNIVERSITY OF MISSOURI AT ROLLA

in partial fulfillment of the requirements for the

Degree of

MASTER OF SCIENCE, METALLURGICAL ENGINEERING

Rolla, Missouri

1964

---

*H. P. Leighty* Approved by  
(advisor) *Paul F. May*  
*R. A. Schaefer* *W. S. Dancy*

## ABSTRACT

A potentiometer and galvanometer setup was used to obtain electrical resistivity data for polycrystalline zinc. Cold working textures were investigated by the reflection technique with a quadrant x-ray spectrometer.

Resistivity data were obtained for specimens that were reduced up to forty per cent from the as received condition, and the corresponding textures were studied. The results indicated that the resistivity change in the rolling direction is due to the reorientation of the c-axis in the rolling caused by cold working.

## ACKNOWLEDGMENTS

The author wishes to express his appreciation to the Ball Brothers Research Corporation for their financial assistance and materials supplied during this investigation. Special thanks are due to Mr. R. A. Kibler, Chief Metallurgist, for making the author's visit to the Ball Brothers' facilities at Muncie, Indiana both enjoyable and enlightening.

The author is also indebted to Dr. H. P. Leighly, Jr. and Prof. R. V. Wolf for their support and advice during the course of this study.

## TABLE OF CONTENTS

	Page
ABSTRACT . . . . .	ii
ACKNOWLEDGMENTS . . . . .	iii
TABLE OF CONTENTS . . . . .	iv
LIST OF ILLUSTRATIONS . . . . .	v
LIST OF TABLES . . . . .	vi
I. INTRODUCTION . . . . .	1
II. REVIEW OF LITERATURE . . . . .	2
A. Electrical Resistivity . . . . .	2
B. Preferred Orientation . . . . .	3
C. Pole Figure Determination . . . . .	5
III. EXPERIMENTAL PROCEDURE . . . . .	7
A. Sample Preparation . . . . .	7
B. Resistivity Measurements . . . . .	7
C. Calculation of Resistivity . . . . .	12
IV. EXPERIMENTAL RESULTS . . . . .	20
A. Theory of Textures in Hexagonal Close Packed System . . . . .	20
B. Experimental Results of Texture . . . . .	22
C. Electrical Resistivity . . . . .	27
V. DISCUSSION AND CONCLUSIONS . . . . .	33
A. Orientation Effects on Resistivity . . . . .	33
B. Defect Effect on Resistivity . . . . .	34
BIBLIOGRAPHY . . . . .	35
APPENDIX A . . . . .	37
APPENDIX B . . . . .	41
VITA . . . . .	42

## LIST OF ILLUSTRATIONS

Figures	Page
1. Stanat Rolling Mill . . . . .	8
2. Resistivity Apparatus and Cooling System . .	10
3. Schematic of Resistivity Apparatus . . . . .	11
4. (0001) Pole Figure of As Received Zinc . . .	24
5. (0001) Pole Figure of 15% Reduced Zinc . . .	25
6. (0001) Pole Figure of 30% Reduced Zinc . . .	26
7. Resistivity Change for Current Flow in Rolling Direction . . . . .	30
8. Resistivity Change for Current Flow in Rolling Direction . . . . .	31
9. Resistivity Change for Current Flow in Transverse Direction . . . . .	32
10. Sample Holder for Reflection Technique and Quadrant Spectrometer . . . . .	38

## LIST OF TABLES

Table	page
I. Resistivity Measurements and Dimensions for Specimen with Current Flow in Rolling Direction . . . . .	14
II. Resistivity Measurements and Dimensions for Specimen with Current Flow in Transverse Direction . . . . .	18

## I. INTRODUCTION

A study of the effect of orientation of certain crystallographic axes on the electrical resistivity is presented in this thesis. Also a brief study was made on the effect of physical defects on the electrical resistivity.

This investigation was made to study the problem of anisotropic properties of non-cubic metals that are subject to cold working. Electrical properties of such metals that are cold worked will vary with crystallographic direction. In electrical components it is usually specified that the materials used must be of non-directional properties. This may also be true in non-cubic materials to be cold worked in any manner.

The electrical resistivity is a good indicator of how other physical properties have been affected by cold working. A study of the effect of reorientation of grains in zinc on the electrical resistivity was therefore undertaken.



## II. REVIEW OF LITERATURE

### A. Electrical Resistivity

The electrical resistivity of metals is caused by the scattering of the electrons by thermal oscillation of the atoms in the lattice, physical defects, and chemical impurities. Also in non-cubic metals the orientation of certain crystallographic axes has an effect on the electrical resistivity. Therefore, zinc, being hexagonal close packed, was studied in sheet form; it was cold rolled so that the effects of crystallographic orientation could be determined and a brief study made on the effects of physical defects.

In 1931, E. P. T. Tyndall and A. G. Hoyem<sup>(1)</sup> studied the effects of orientation of zinc single crystals on the resistivity and found that they followed the Voigt-Thomson symmetry relationship which states that the resistivity of zinc crystals is a linear function of the square of the cosine of the angle of orientation which is the angle between the direction of current flow and the main ( $\bar{c}$ ) crystallographic axis. Later in 1932 Poppy<sup>(2)</sup> repeated this experiment using single crystals of zinc of varying purity and found that only in high purity crystals was this relationship true and that the application of a minor stress caused some variation.

In 1942 Koehler and Seitz<sup>(3)</sup> reported the effect of cold working on the resistivity in copper and calculated the change introduced by Taylor dislocations. Later in

1948 Koehler recorded an orientation dependence of the dislocation effect in copper single crystals caused by the angle between the current flow and the single crystals<sup>(4)</sup>.

Matthiessen's rule<sup>(5)</sup> states that the increase in electrical resistivity introduced by thermal vibration of the lattice due to increase in temperature is independent of the (small) amount of alloying elements present and the deformation state. The reverse is also true and indicates that the plots of total resistivity for various alloy levels versus temperature should all have the same slope.

The independent effects of impurities and physical defects on the resistivity in copper were reported by Kunzler<sup>(6)</sup> in 1961. Kunzler indicated his results for both single crystals and polycrystalline materials. Wintenberger<sup>(7)</sup> studied the effects of impurities on electrical resistivity changes introduced by vacancies and dislocations in aluminum. He reports that the number of vacancies produced by deformation is independent of the impurity level while there is a dependence of resistivity caused by dislocations. This may be interpreted to indicate that impurities limit the size of dislocation rings.

#### B. Preferred Orientation

Preferred orientation is indicated when grains tend to assume some particular orientation, where random orientation does not exhibit this. This preference can be better indicated by x-ray diffraction<sup>(8)</sup> than a film technique. The x-ray diffraction technique quantitatively

measures intensity which is used to plot the pole figure. A comparison of pole figures is used to determine the degree of preferred orientation.

In cold-rolled sheet it is found that grains are so oriented that a particular direction in a plane tends to be parallel to the rolling direction and the sheet surface, while in cold-drawn wire a specific crystallographic direction in most grains is parallel to the fiber or wire axis<sup>(8)</sup>. The cold drawn grains can have any rotational position about the fiber axis. In sheet there is less symmetry and the grains do not have a common crystallographic direction with which they can have any rotational position relationship.

The slip planes of hexagonal close packed metals upon rolling should be rotated into planes parallel to the surface of the sheet. The texture which predominates is one where the slip plane (basal plane) lies near or in the plane of rolling in metals for closest packing of atoms ( $c/a=1.633$ ).

Calnan and Clews<sup>(9)</sup> described a graphical technique for texture analysis using the combination of the rotational tendency of each slip and twinning tendency in single crystals. They indicated that, upon the applied resolved shear stress attaining the critical value for the most favorably oriented slip system, slip does not need to occur immediately, thus maintaining cohesion of grain boundaries. Here neighboring grains induce constraints upon the deforming grain

and cause a lesser stress so that the critical value is not reached, possibly due to duplex and multiple slip. The texture can be determined by analysis of the associated rotations.

### C. Pole Figure Determination

The methods for determining pole figures by Decker et al. (10) and Schulz (11)(12) use data obtained by a Geiger counter x-ray diffraction spectrometer. Both these methods give high precision results by quantitatively measuring the diffracted x-rays from the crystallographic planes in the sample with Geiger counter.

The transmission method developed by Decker et al. (10) investigated thin samples and a special sample holder was designed to allow rotation about the diffractometer axis and about the horizontal normal to the sample surface. This allows rotation of the reflecting plane pole over the polar plot. The integrated intensity of each position is corrected for absorption of the diffracted beam by the sample and this corrected intensity is then proportional to the pole density at that position on the polar net.

The reflection method developed by Schulz (11)(12) measures the beam intensity which is reflected from the same side of the sample as the incident beam. The sample holder in this case allows for rotation about the normal to the sample surface and a horizontal axis. There must be a correction made for defocusing of the diffracted beam. Only the central portion of the pole figure can be investigated,

but here no absorption correction is needed for tilting angles (revolution angles) between approximately 40 to 90 degrees. Here again the corrected intensity is proportional to the pole density.

In 1952 Williams and Eppelsheimer<sup>(13)</sup> described the modification of the Schulz and Decker techniques for the reflection and transmission procedures for determining preferred orientation. This modified technique is more fully described in Appendix A. The above technique and apparatus was also used by Wilcox<sup>(14)</sup> to determine the cold-rolled textures of cobalt. In this procedure over-lapping is produced in the region of the 30 degree angle of revolution which is used to normalize one set of data and make the two techniques agree with the other sets of data in the region of overlap.

Upon accomplishing this, the intensities which are proportional to pole density can be plotted on the polar net for each position where measurements were made. Then the points of equal intensity on the polar net are connected producing the pole figure. This is the only real quantitative analysis of orientation in materials, while the photographic technique is a qualitative method.

### III. EXPERIMENTAL PROCEEDURE

#### A. Sample Preparation

The zinc sheets received from Ball Brothers Research Corporation were cold rolled in the as received condition without the use of an annealing procedure; the Stanat Rolling Mill, shown in Figure 1, was used for this treatment. Reductions of 0 to 40 per cent were obtained with approximately eight passes in the mill, taking care to avoid any generation of excessive heat; this could cause partial recrystallization which occurs at 43 degrees Celsius in zinc<sup>(15)</sup>. There was a slight amount of lateral dimensional increase, but the major increase was in the longitudinal direction. The sheet edges were trimmed to remove any edge cracks present. Samples for transverse and rolling direction resistivity measurements were obtained by cutting with a shear. Dimensions were obtained by use of micrometer calipers and a rule. The longitudinal dimension was much greater than the width or thickness, so the  $\pm 0.05$  error in the length was assumed to be negligible. The accuracy in the width and thickness was approximately  $\pm 0.002$  and  $\pm 0.001$  respectively. Any sample with noticeable surface defects was discarded as were samples taken near the edges of the sheet.

#### B. Resistivity Measurements

The resistivity measurements were made in a constant temperature bath containing a neutral oil. Temperature was controlled within  $\pm 0.5$  degrees Celsius by use of a

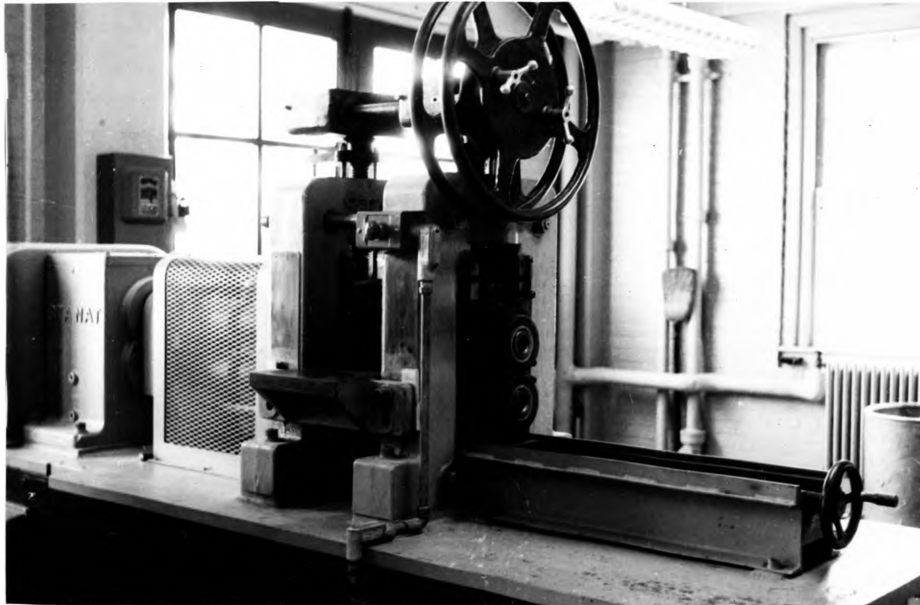


Figure 1. Stanat Rolling Mill

thermoregulator in conjunction with a cooling system as seen in Figure 2. This was to eliminate the effect of the increase in resistivity introduced by the temperature coefficient of electrical resistivity.

Current was supplied to the specimen by a 1.5 volt dry cell with the current being regulated by a rheostat to provide  $960 \pm 5$  milliamps. Point contacts of ground steel at a known distance apart were used to measure the potential drop in the specimen. Figure 3 shows the electrical apparatus.

The galvanometer, which had a sensitivity of  $\pm 0.0016$  amps/millimeter, was balanced by use of a Weston standard cell and a  $K_2$  potentiometer. The throw switch on the potentiometer was put in the "emf" position to measure the potential drop in the specimen. The galvanometer was then balanced against the "emf" by use of the slide wire of the potentiometer. Upon balancing of the galvanometer the potential drop could be read directly and any current passing from the specimen to the potentiometer was effectively zero. Six potential measurements were taken of each sample in this manner and averaged to obtain the final "emf" value.

Some of the difficulties encountered were:

1. The sensitivity of the galvanometer was much greater than that of the potentiometer and resulted in only a rough balancing of the galvanometer against the standard cell. It was felt that the use of a more



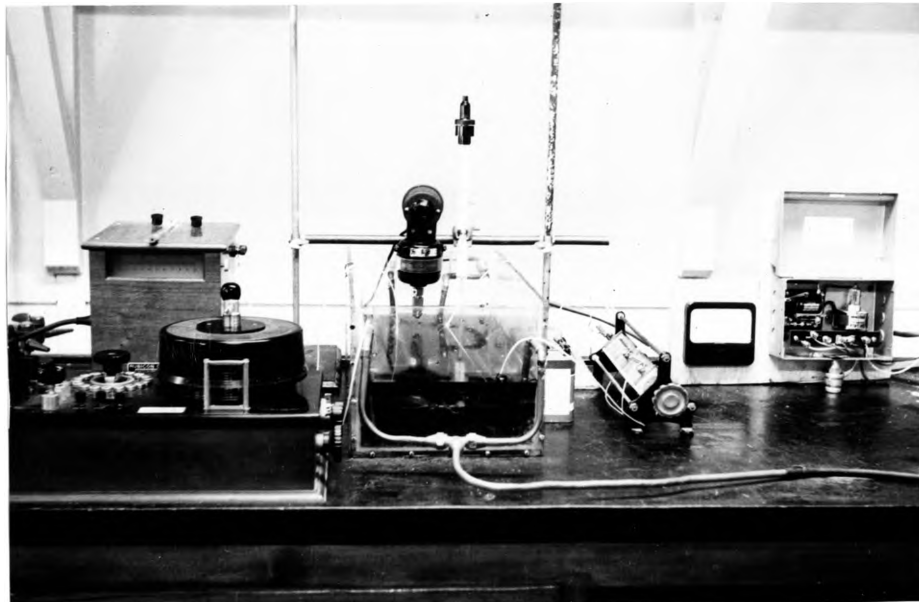
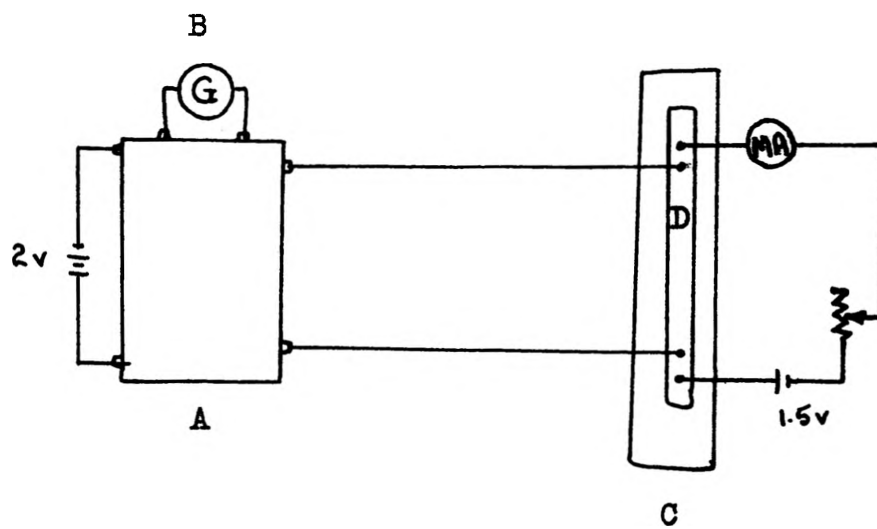


Figure 2. Resistivity Apparatus and Cooling System



A Potentiometer & Standard Cell      C Temperature Tank  
B Galvanometer                              D Specimen

Figure 3. Schematic of Resistivity Apparatus

accurate potentiometer and a less antiquated standard cell would have improved this situation.

2. Irregularities of the resistivity between samples of approximately the same reduction were probably caused by difficulties in dimensional measurements. This could have been eliminated by the use of the density method of determining cross-sectional area mentioned by Tyndall and Hoyem(1).

3. The current supplied to the specimen had to be repeatedly checked to insure that it was held constant. This was probably due to the rheostat not being sensitive enough to produce a constant current.

4. Variations in potential measurements resulted from the above mentioned items plus the fact that the galvanometer was subject to disturbance by the slightest mechanical shock.

5. The use of a Kelvin Double Bridge would have given much better accuracy than the potentiometer.

#### C. Calculation of Resistivity

In calculating the electrical resistivity of the sheet zinc the following equation was used:

$$p = \frac{VA}{IL}$$

where:

p = electrical resistivity in  $\mu\Omega$ -cm,

V = potential drop in the specimen,  $\mu$ v,

A = cross-sectional area in square centimeters,

I = current flowing through the specimen in amps,

L = distance between potential contacts in centimeters.

No compensation was made in the final resistivity values for temperature as it was assumed to cause an error of less than  $\pm 0.002 \mu\Omega\text{-cm}$ . The average values for resistivity are shown for the transverse and rolling directions in Tables I and II.

TABLE I

RESISTIVITY MEASUREMENTS AND DIMENSIONS FOR  
SPECIMEN WITH CURRENT FLOW IN ROLLING DIRECTION

Specimen	Av. Thickness (in.)	Av. Width (in.)	Length (in.)	Amperes	Millivolts	Resistivity ( $\mu\Omega$ - cm.)
As Rec'd	.0575	.4020	9.0	2.10	1.9068	5.993
	.0560	.4000	9.0	2.10	1.9657	6.187*
	.0578	.4050	9.0	2.10	1.8974	5.959
	.0579	.4040	9.0	2.10	1.9051	5.987
	.0580	.4061	9.0	2.10	1.9529	6.181*
	.0572	.4056	9.0	2.10	1.9180	5.996
						Av. 5.984
6% Red.	.0541	.4610	10.0	0.96	0.9327	6.155*
	.0540	.4590	10.0	0.96	0.9300	6.099*
	.0538	.4596	10.0	0.96	0.9259	6.057
	.0540	.4541	10.0	0.96	0.9353	6.068
	.0544	.4548	10.0	0.96	0.9371	6.134*
	.0542	.4563	10.0	0.96	0.9402	6.152*
	.0540	.4550	10.0	0.96	0.9309	6.052
						Av. 6.060
12% Red.	.0502	.4010	9.0	2.05	2.1281	5.750*
	.0505	.4025	9.0	2.10	2.1467	5.865*
	.0508	.4078	9.0	2.10	2.1883	6.092
	.0505	.4110	10.0	2.10	2.3984	6.030
	.0505	.4068	10.0	2.10	2.4183	6.009

\* These values of resistivity not used due to various errors.

TABLE 1 (Cont'd)

<u>Specimen</u>	<u>Av. Thickness (in.)</u>	<u>Av. Width (in.)</u>	<u>Length (in.)</u>	<u>Amperes</u>	<u>Millivolts</u>	<u>Resistivity (<math>\mu\Omega</math>-cm.)</u>
12% Red. (cont'd)	.0504	.4117	10.0	2.10	2.4835	6.237
						Av. 6.105
14% Red.	.0479	.4382	10.0	0.96	1.1139	6.196*
	.0476	.4357	10.0	0.96	1.1126	6.112
	.0475	.4368	10.0	0.96	1.1121	6.103
	.0475	.4380	10.0	0.96	1.1118	6.120
	.0478	.4379	10.0	0.96	1.1119	6.158*
						Av. 6.112
15% Red.	.0480	.4431	10.0	0.96	1.0785	6.069*
	.0482	.4427	10.0	0.96	1.0814	6.105
	.0482	.4425	10.0	0.96	1.0824	6.108
	.0483	.4420	10.0	0.96	1.0822	6.113
	.0480	.4425	10.0	0.96	1.0863	6.105
	.0476	.4418	10.0	0.96	1.0827	6.024*
						Av. 6.107
20% Red.	.0450	.4408	10.0	0.96	1.1635	6.106
	.0447	.4414	10.0	0.96	1.1721	6.119
	.0448	.4400	10.0	0.96	1.1700	6.102
	.0448	.4415	10.0	0.96	1.1648	6.096*
	.0449	.4403	10.0	0.96	1.1752	6.147*
	.0450	.4409	10.0	0.96	1.1654	6.118
						Av. 6.111

\* These values of resistivity not used due to various errors.

TABLE 1 (Cont'd)

<u>Specimen</u>	<u>Av. Thickness (in.)</u>	<u>Av. Width (in.)</u>	<u>Length (in.)</u>	<u>Amperes</u>	<u>Millivolts</u>	<u>Resistivity (<math>\mu\Omega</math>-cm.)</u>
21% Red.	.0458	.3775	10.0	0.96	1.3346	6.105
	.0458	.3785	10.0	0.96	1.3357	6.126
	.0452	.3800	10.0	0.96	1.3545	6.156
	.0460	.3788	10.0	0.96	1.3396	6.176*
	.0456	.3800	10.0	0.96	1.3469	6.175*
	.0455	.3788	10.0	0.96	1.3513	6.162*
	.0460	.3795	10.0	0.96	1.3336	6.160*
						Av. 6.130
22.5% Red.	.0450	.4380	8.0	0.96	0.9430	6.147
	.0447	.4391	8.0	0.96	0.9373	6.084*
	.0449	.4376	8.0	0.96	0.9368	6.093*
	.0448	.4390	8.0	0.96	0.9347	6.079*
	.0448	.4410	8.0	0.96	0.9365	6.119
						Av. 6.133
24% Red.	.0442	.4593	10.0	0.96	1.1377	6.111
	.0441	.4618	10.0	0.96	1.1114	5.989*
	.0440	.4616	10.0	0.96	1.1376	6.113
	.0430	.4633	10.0	0.96	1.1509	6.066*
	.0441	.4601	10.0	0.96	1.1361	6.099*
	.0436	.4613	10.0	0.96	1.1562	6.153
	.0443	.4608	10.0	0.96	1.1264	6.084*
						Av. 6.126

\* These values of resistivity not used due to various errors.

TABLE 1 (Cont'd)

<u>Specimen</u>	<u>Av. Thickness (in.)</u>	<u>Av. Width (in.)</u>	<u>Length (in.)</u>	<u>Amperes</u>	<u>Millivolts</u>	<u>Resistivity (<math>\mu\Omega</math>-cm.)</u>
28.5% Red.	.0407	.4380	10.0	0.96	1.2987	6.125
	.0412	.4405	10.0	0.96	1.2802	6.147
	.0413	.4371	10.0	0.96	1.2851	6.138
	.0406	.4375	10.0	0.96	1.3076	6.145
	.0408	.4395	10.0	0.96	1.2915	6.127
						Av. 6.136
40% Red.	.0338	.4405	10.0	0.96	1.5552	6.126
	.0339	.4416	10.0	0.96	1.6006	6.340*
	.0337	.4406	10.0	0.96	1.5560	6.113
	.0339	.4401	10.0	0.96	1.5550	6.138
	.0339	.4425	10.0	0.96	1.5563	6.177*
						Av. 6.126

\* These values of resistivity not used due to various errors.



TABLE II

RESISTIVITY MEASUREMENTS AND DIMENSIONS FOR  
SPECIMEN WITH CURRENT FLOW IN TRANSVERSE DIRECTION

<u>Specimen</u>	<u>Av. Thickness (in.)</u>	<u>Av. Width (in.)</u>	<u>Length (in.)</u>	<u>Amperes</u>	<u>Millivolts</u>	<u>Resistivity (<math>\mu\Omega</math>-cm.)</u>
As Rec'd	.0590	.4390	6.0	0.96	0.5267	6.016
	.0585	.4363	6.0	0.96	0.5325	5.993
	.0595	.4365	6.0	0.96	0.5278	6.086*
	.0590	.4368	6.0	0.96	0.5326	6.053*
	.0587	.4380	6.0	0.96	0.5302	6.011
						Av. 6.004
17% Red.	.0478	.4410	5.0	0.96	0.5444	6.048
	.0486	.4425	5.0	0.96	0.5434	6.189*
	.0479	.4398	5.0	0.96	0.5431	6.059
	.0478	.4390	6.0	0.96	0.6570	6.079
						Av. 6.052
15% Red.	.0478	.4400	5.0	0.96	0.5368	5.974*
	.0480	.4415	5.0	0.96	0.5365	6.016
	.0480	.4375	5.0	0.96	0.5428	6.032
	.0480	.4410	5.0	0.96	0.5365	6.010
						Av. 6.019
20% Red.	.0445	.4415	5.0	0.96	0.5827	6.058
	.0442	.4418	5.0	0.96	0.5833	6.027*
	.0445	.4420	5.0	0.96	0.5805	6.042
	.0442	.4415	5.0	0.96	0.5811	6.001*

\* These values of resistivity not used due to various errors; these errors are discussed on pages 11 and 12.

TABLE 2 (Cont'd)

<u>Specimen</u>	<u>Av. Thickness (in.)</u>	<u>Av. Width (in.)</u>	<u>Length (in.)</u>	<u>Amperes</u>	<u>Millivolts</u>	<u>Resistivity (<math>\mu\Omega</math>-cm.)</u>
20% Red. (Cont'd)	.0445	.4418	5.0	0.96	0.5808	6.042
						Av. 6.047
21% Red.	.0456	.3827	5.0	0.96	0.6664	6.154*
	.0451	.3801	5.0	0.96	0.6705	6.082
	.0450	.3797	5.0	0.96	0.6725	6.081
						Av. 6.081
23.5% Red.	.0447	.4380	5.0	0.96	0.5866	6.077
	.0447	.4335	5.0	0.96	0.5958	6.109
	.0445	.4372	5.0	0.96	0.5851	6.024
	.0452	.4381	5.0	0.96	0.5873	6.154*
						Av. 6.069
29% Red.	.0410	.4410	5.0	0.96	0.6326	6.043
	.0413	.4478	5.0	0.96	0.6310	6.175*
	.0411	.4450	5.0	0.96	0.6301	6.098
	.0412	.4445	5.0	0.96	0.6285	6.091
	.0410	.4418	5.0	0.96	0.6270	6.010
						Av. 6.098
40% Red.	.0335	.4420	5.0	0.96	0.7867	6.164*
	.0337	.4405	5.0	0.96	0.7763	6.098
	.0335	.4415	5.0	0.96	0.7771	6.082
	.0335	.4401	5.0	0.96	0.7831	6.110
	.0335	.4390	5.0	0.96	0.7822	6.087
						Av. 6.094

\* These values of resistivity not used due to various errors.

#### IV. EXPERIMENTAL RESULTS

##### A. Theory of Textures in Hexagonal Close Packed System

In a space lattice, the planes of highest atomic density generally have the lowest resistance to shearing stress and are usually the preferred slip planes. The same general assumption also applies to twinning where the shearing force acts parallel to the twin plane and atomic movement is in that direction also. As far as atomic movement is concerned, twinning can most generally be considered as a homogeneous slipping, where the atomic movement generally is parallel to the twin plane. The direction of slip is coincident with the most closely packed rows of atoms in the slip plane.

Upon the application of a stress, the lattice must then rotate to accommodate the stress so that the normal to the slip plane moves towards the compression axis and the slip plane direction toward the tensile axis.

However, polycrystalline materials are more complex as neighboring grains restrain each other; one must then assume that multiple deformation mechanisms occur simultaneously to avoid grain boundary separation. This demands multiple slip and suppresses some other deformation mechanisms that occur where there are no grain boundary restraints. The stress on a certain lattice is not necessarily the same as the applied stress, and the difference is caused by the stresses from adjacent material acting on the lattice.

Under cold rolling conditions, there is a rolling direction deformation due to the tensile stress and in the transverse direction due to a compressive stress. Here only mechanisms which bring reduction in the thickness are assumed to be in operation.

The usual slip system in zinc is (0001) and the basal plane (0001) slips in a  $[11\bar{2}0]$  resulting in a slip rotation so that the  $[11\bar{2}0]$  coincides with the rolling direction. The basal slip also causes the (0001) to be rotated into the rolling plane as the deformation continues. As this occurs  $\{10\bar{1}2\}$  type twinning can and does occur causing the material to lengthen in the tensile direction; further reorientation of the basal plane takes place so that the basal plane normal lies at approximately 60 degrees from the rolling plane normal allowing further slip.

Furthermore, zinc would appear to be quite ductile in that these two mechanisms, basal slip and  $\{10\bar{1}2\}$  twinning, are complimentary; each rotating the lattice into a desirable position for the other. However, with only compressive twinning accounting for deformation other than in the rolling direction, and this accounting for only a small amount of deformation at the most; the material may easily fail as a result of intergranular separation.

It might be expected that zinc might not have a well defined terminal texture as a result of the continuous

movement of the basal poles, but normally the greatest concentration is found to be 20 to 25 degrees from the normal to the rolling plane in the rolling direction<sup>(16)</sup>. The orientation is almost intermediate between the theoretical position of the basal plane and that of the theoretical position for twinning that takes place at 60 degrees in the rolling direction.

#### B. Experimental Results of Textures

As previously mentioned, the only method for determining the amount of preferred orientation is by x-ray techniques. Therefore, the pole figures were obtained for the (0001) by the reflection technique. The pole figure for the (0001) of the as received material is shown in Figure 4. It can be seen that the greatest pole density lies between 30 and 40 degrees from the pole center in the rolling direction. The pole figures for the (0001) of the materials that were reduced 15 and 30 per cent are shown in Figures 5 and 6; it can be seen that the greatest pole densities are at approximately 50 degrees from the pole center in the rolling direction.

Although no exact figures can be placed on the preferred orientation of these samples, it can be seen from the pole figures that, as the amount of reduction increases, the (0001) pole densities move toward the rolling direction, and the greatest density occurs between 40 and 50 degrees from the rolling plane normal.

This increasing shift of pole densities toward the rolling direction with increasing reduction by cold rolling is a result of slip of the basal plane (0001) in the  $[11\bar{2}0]$  direction. Also  $\{10\bar{1}2\}$  type twinning occurs reorienting the (0001) and allows further slip. These mechanisms tend to shift the maximum of the pole densities toward the pole center and result in a concentration at 25 degrees in the rolling direction at 95 per cent reduction. The experimental results show a concentration at 35 degrees, and thus it is assumed that greater reductions would shift the maximum pole densities toward the pole center to coincide with the results reported by Barrett<sup>(16)</sup> .

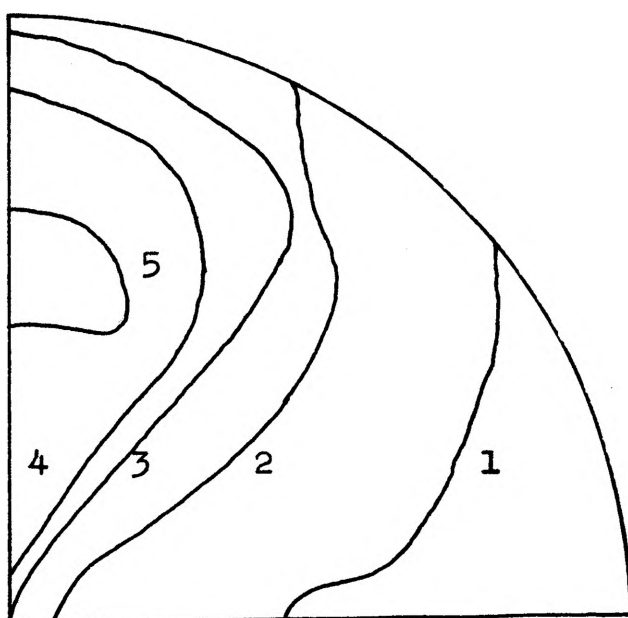


Figure 4. (0001) Pole Figure of As Received Zinc

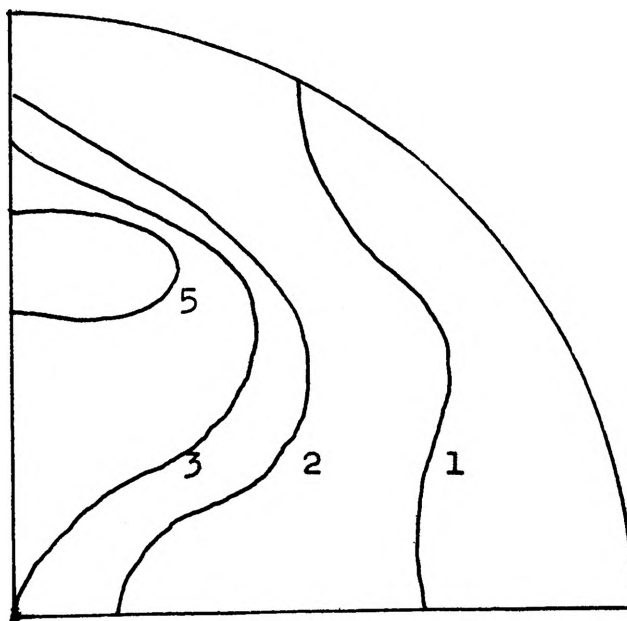


Figure 5. (0001) Pole Figure of 15% Reduced Zinc



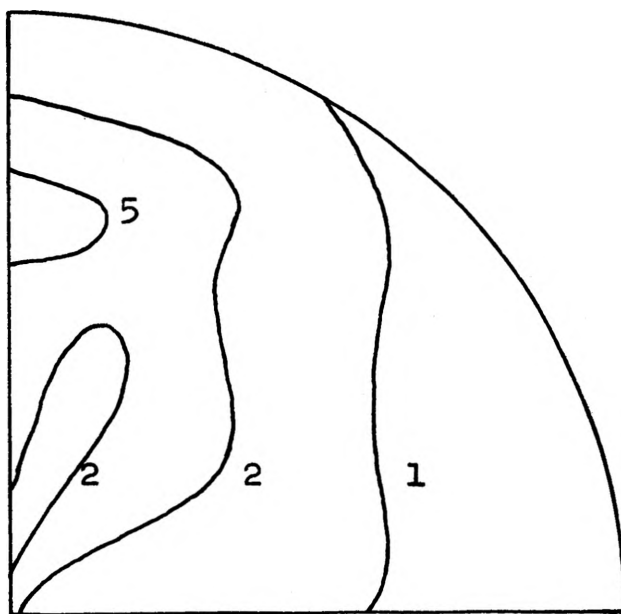


Figure 6. (0001) Pole Figure of 30% Reduced Zinc

## C. Electrical Resistivity

The electrical resistivity can be broken into three elements according to Kunzler<sup>(6)</sup>.

$$\rho = \rho_{\text{therm}} + \rho_{\text{phys}} + \rho_{\text{chem}}$$

where:

$\rho$  is the total electrical resistivity in  $\mu\Omega\text{-cm}$ ,

$\rho_{\text{therm}}$  is resistivity due to thermal oscillation of atoms in the lattice in  $\mu\Omega\text{-cm}$ ,

$\rho_{\text{phys}}$  is the resistivity introduced by electron scatter from physical defects in  $\mu\Omega\text{-cm}$ ,

$\rho_{\text{chem}}$  is the resistivity resulting from chemical impurities in the structure.

Koehler<sup>(3)</sup> neglects the  $\rho_{\text{chem}}$  term. The views of his work are incorporated in this thesis, assuming that impurities present would have very little effect, as the same approximate composition was assumed for all of the zinc sheet used. Kunzler's work<sup>(6)</sup> appears to support this view when he shows that the maximum resistivity due to impurities in copper accounts for only 1% of the total resistivity. The effects of both impurities and defects are shown in the table below.

### Chemical Impurities and Defects Effect in Copper<sup>(6)</sup>

Impurity	$\Delta\rho/\text{at.}\%$ impurity	Defect	$\Delta\rho/\%$ defect
Ag	0.2 $\mu\Omega\text{-cm}/\%$	Vacancies	1.3 $\mu\Omega\text{-cm}/\%$
Ni	2.0	Interstitials	5.0
Sn	5.0	Dislocations	$3 \times 10^{-4} N$
Sb	9.0		

where N is equal to  
cm of dislocation  
 cubic cm

Koehler<sup>(3)(4)</sup> reports that the increase in electrical resistance (calculated and observed) resulting from physical defects introduced by cold working of copper at room temperature ranges from 0.4 to 3.0 per cent. Furthermore he found that the resistivity produced by cold working increased approximately linearly with the density of dislocations<sup>(4)</sup>.

It was further assumed that the effects of physical defects in zinc would be constant over the range of cold working with a possible increase at the initial reductions. Also since the basal plane is the slip plane with  $[11\bar{2}0]$ , the slip direction, and assuming edge-type dislocations, the effect of the defects on resistivity change in the rolling direction would become smaller as the c-axis moves toward the rolling direction. It is felt that edge-type dislocations would contribute more to the resistivity change in the direction perpendicular to the rolling direction.

It is considered here that the increase in the electrical resistivity in the rolling direction for zinc is due mainly to the preferred orientation of the c-axis toward the rolling direction. This increase is caused by the fact that the resistivity value for the c-axis is greater than in any other direction. It was reported by Poppy<sup>(2)</sup> that the resistivity for the c-axis is 6.161  $\mu\Omega$ -cm and 5.842  $\mu\Omega$ -cm along the hexagonal axes. Therefore, it is suggested that the total resistivity is equal to

$p_{\text{therm}} + p_{\text{orient}}$  where  $p_{\text{orient}}$  is the change introduced by the reorientation of the c-axis toward the rolling direction.

In the transverse direction there is no preferred orientation effect and any increase in resistivity should be accounted for by physical defects as noted previously. Therefore, the equation, total resistivity is equal to  $p_{\text{therm}}$  plus  $p_{\text{phys}}$ , is assumed to represent the resistivity in the transverse direction.

The results shown in Figures 8 and 9 indicate that the increase in resistivity in the rolling direction and the transverse direction over the as received condition is 2.68% and 0.90% respectively with cold rolling reductions up to 40 per cent. However, if the value for the resistivity of a random orientation is used, the increase accounts for 3.71% in the rolling direction and 2.33% in the transverse.

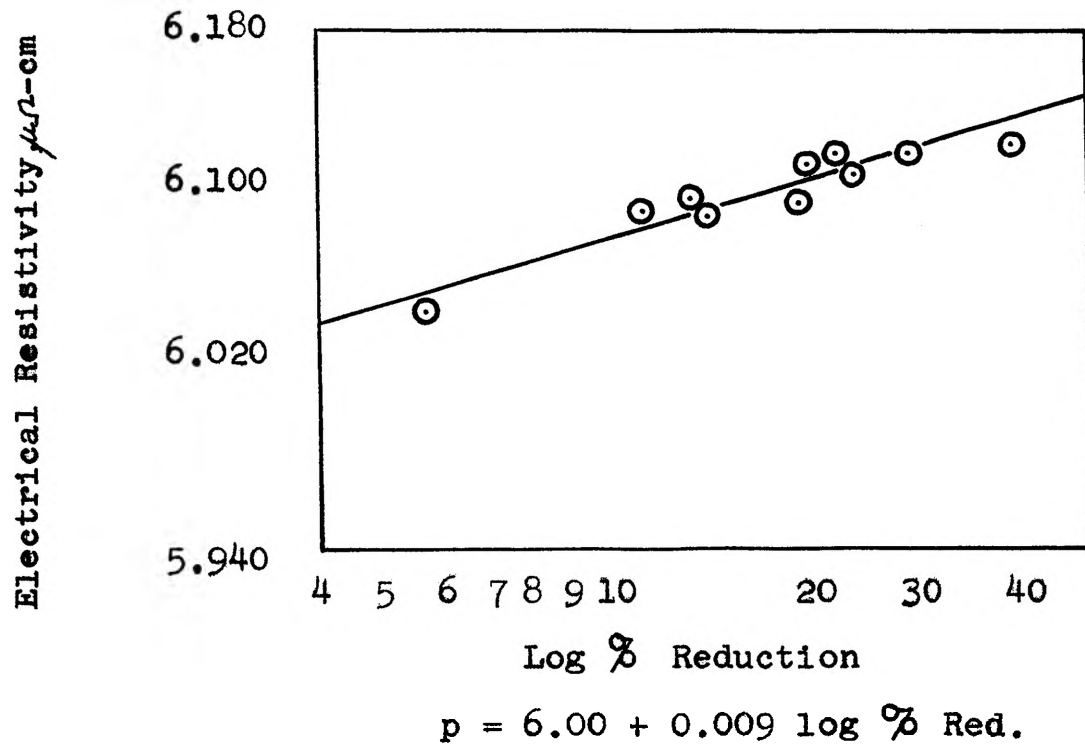


Figure 7. Resistivity Change for Current Flow in Rolling Direction

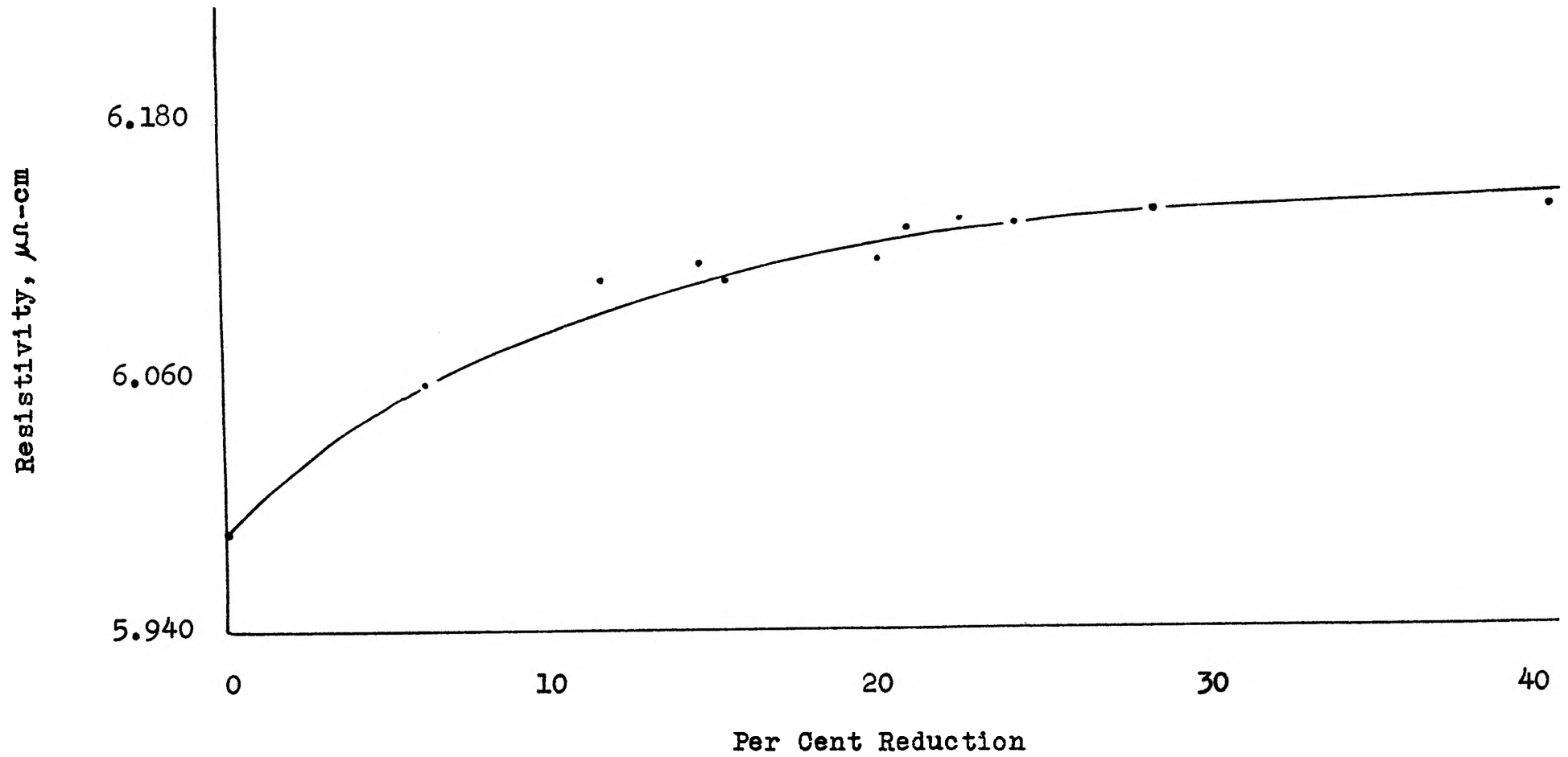


Figure 8. Resistivity Change for Current Flow in Rolling Direction

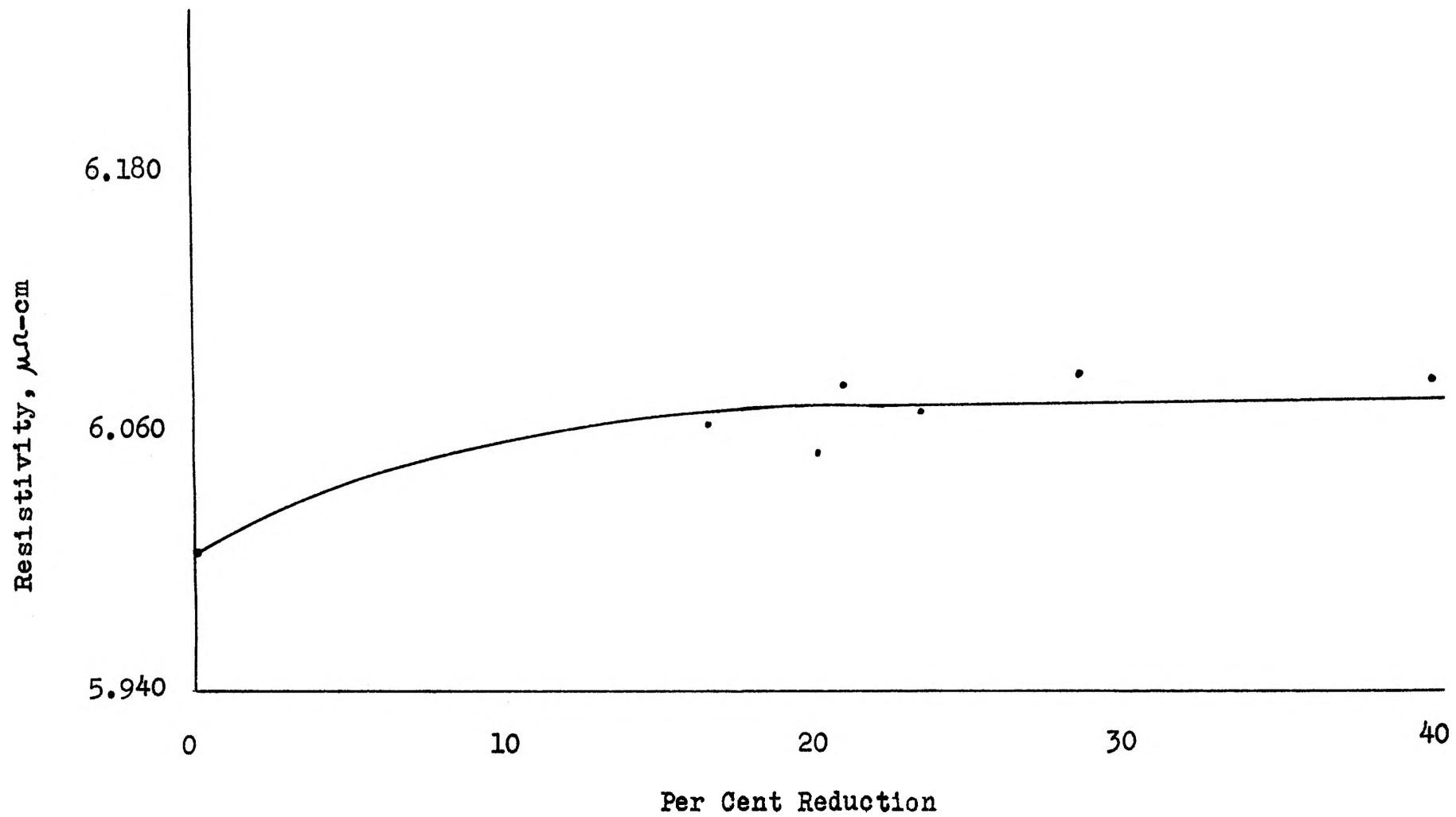


Figure 9 . Resistivity Change for Current Flow in Transverse  
Direction

## V. DISCUSSION AND CONCLUSIONS

### A. Orientation Effects on Resistivity

The results of the investigation of the effect of reduction by cold rolling on resistivity in the rolling direction are shown in Figure 8. A plot of resistivity versus the log of the per cent reduction, Figure 7, gave a straight line; this indicates that the reduction effect is continuous through all amounts of reduction and results in a continuous increase in resistivity with reductions up to forty per cent. The equation of the graph can be expressed for reductions up to forty per cent as follows:

$$\text{Electrical resistivity} = 6.00 + 0.009 (\log \% \text{ reduction}).$$

In perfect preferred orientation, the basal plane is oriented parallel to the rolling plane, and the c-axis is normal to the rolling direction. This perfect preferred orientation was not observed; however, with greater reductions this should become more prevalent. As is reported, the increasing concentration of the basal pole is at 35 degrees from the rolling plane normal, and the greatest density of the c-axis is at an angle of  $55^{\circ}$  to the rolling direction accounting for the resistivity increase.

Above forty per cent reduction the resistivity remains nearly constant, and it is assumed the preferred orientation remains approximately the same. This is based on the small difference between the preferred orientation of the as received material and the sheet after 30 per cent



reduction. Also, the maximum in resistivity should be near  $6.16 \mu\Omega\text{-cm}$  along the c-axis, and the resistivity is  $6.14 \mu\Omega\text{-cm}$  after a 40 percent reduction; therefore, only a very slight increase would result in further reductions.

#### B. Defect Effect on Resistivity

The resistivity change in the transverse direction introduced by cold rolling is shown in Figure 9. This increase is not a result of reorientation of the crystallographic grains in the specimen as no preference is found in any rotational position about the rolling direction as well as in the transverse direction. Also, the resistivity is the same along all three basal axes and, therefore, the increase found was assumed to be caused by physical defects introduced by cold rolling.

As the basal plane is the slip plane, this would be the plane of highest dislocation density. Koehler<sup>(4)</sup> found that the resistivity increases approximately linearly with an increase in dislocation density and that dislocation density increases with the amount of cold rolling. As a result of this, it was felt that the dislocations caused scattering of electrons in the transverse direction.

## BIBLIOGRAPHY

1. TYNDALL, E. P. T. and HOYEM, A. G. (1931) Resistivity of Single Crystal Zinc. Phys. Rev. Vol 38, p. 820.
2. POPPY, W. J. (1943) Electrical Resistivities of Single and Optically Mosaic Zinc Crystals. Phys. Rev. Vol 46, p. 815.
3. KOEHLER, C. W. (1942) A Calculation of the Increase in Electrical Resistance Produced by Cold Working. Phys. Rev. Vol 61, p. 390.
4. KOEHLER, C. W., and SEITZ, F. (1949) A Calculation of Changes in Conductivity of Metals Produced by Cold Working, Phys. Rev., Vol 75, p. 106.
5. DOAN, G. E. (1953) The Principles of Physical Metallurgy. p. 53.
6. KUNZLER, J. E. (1961) Electrical Properties of Metals and the Importance of Purity. Ultra-High-Purity Metals. p. 171.
7. WINTENBERGER, M. (1957) Compt. Rend. Acad. Sci. Vol 242, p. 2800.
8. CULLITY, B. D. (1956) Elements of X-Ray Diffraction. p. 285.
9. CALNAN, E. A. and CLEWS, C. J. B. (1951) Development of Deformation Textures in Metals -- Hexagonal Close Packed System. Phil. Mag. Vol 42, p. 919.
10. DECKER, B. F., ASP, E. T. and HARKER, D. (1945) Preferred Orientation Determination Using a Geiger Counter X-Ray Diffraction Goniometer. J. Appl. Phy. Vol 14, p. 388.
11. SCHULZ, L. G. (1949) A Direct Method of Determining Preferred Orientation of a Flat Reflection Sample Using a Geiger Counter X-Ray Spectrometer. J. Appl. Phy. Vol 20, p. 1030.
12. SCHULZ, L. G. (1949) Determination of Preferred Orientation in Flat Transmission Samples Using a Geiger Counter X-Ray Spectrometer. J. Appl. Phy. Vol 20, p. 1033.

13. WILLIAMS, D. N. and EPPELSHEIMER (1952) Universal Specimen Mount for Pole Figure Determination Using the Schulz-Decker Technique. University of Missouri Bulletin.
14. WILCOX, R. C. (1962) An Investigation of the Deformation Textures of Cobalt. Ph. D. Dissertation University of Missouri Appendix A.
15. SMITH, R. A. (1963) An Electrolytic Polishing and Recrystallization Study of Zinc and Zinc Alloys. M. S. Thesis University of Missouri p. 24.
16. BARRETT, C. S. (1952) Structure of Metals. p. 519.

## APPENDIX A

### A. X-Ray Diffraction Technique

As mentioned previously the apparatus and procedure developed by Williams and Eppelsheimer<sup>(13)</sup> were used extensively in this investigation of the rolling textures of zinc sheet. This particular method allows the entire pole figure to be determined and is much faster than using both the Schulz and Decker techniques. The sample holder and quadrant spectrometer are shown in Figure 10.

More consistent data were obtained by averaging two intensity readings at each angle of revolution and rotation. In order to obtain the correct Bragg angle value of intensity, intensity readings were taken by letting the Geiger counter move over an approximately five degree range. Actual intensity measurement was made by measuring the area under the intensity peak with a planimeter. It was felt this gave better accuracy than the peak height method. The intensity which had been corrected for defocusing in the reflection portion was plotted on the polar net.

The centering of the sample on the stage of the sample holder for reflection intensity measurements was accomplished by recording the intensities at 0, 30, 60, and 90 degrees of rotation at the polar center. The sample was then remounted until the readings were the same at all angles of rotation at the polar center.

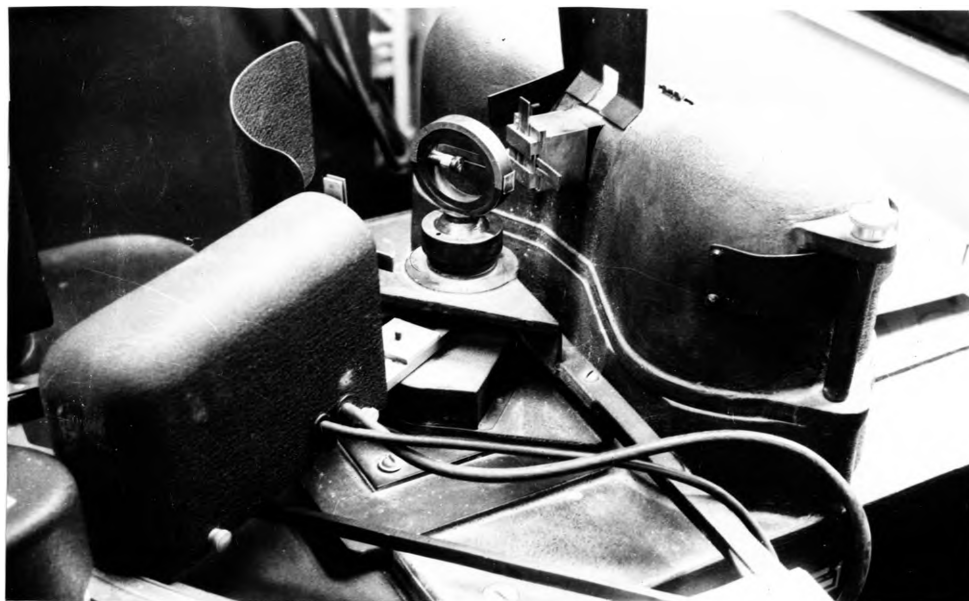


Figure 10. Sample Holder for Reflection Technique and  
Quadrant Spectrometer

The slit system for the reflection method involved the use of a horizontal slit at the sample holder and a vertical slit at the x-ray tube. This resulted in a square beam hitting the sample and permits a rectangular specimen to be used. It was felt that the slit for the sample holder could be improved by redesigning it so that it would fit permanently and could be adjusted by set screws. The positioning of the slit could be accomplished by use of a fluorescent screen. This would eliminate any displacement of the horizontal slit and eliminate the resulting errors in intensity readings. In this experiment the horizontal slit was repositioned until it did not cause variation in the intensity readings at the pole center and then was glued in position.

#### B. Defocusing Error Corrections

The defocusing in the reflection portion is a result of portions of the irradiated area of the sample moving out of the focusing circle, which is described by the sample surface, the radiation source and the receiving slit. This defocusing effect occurs as the sample is revolved and causes a decrease in the intensity as the angle of revolution moves away from the center of the pole figure.

In order to limit the effect of defocusing, an annealed zinc powder sample of minus 325 mesh size was analyzed at each angle of rotation and revolution that were to be used in the texture determination. The

average of two measurements for the (0001) line was made to obtain a better result at each angle. The intensities at each angle of revolution were averaged and divided into the intensity for the center of the pole figure. These ratios were used to correct the intensity readings at each angle of revolution in the textures studies and are listed below.

Angle of Revolution	Correction Factor
90	1.00
80	1.00
70	1.02
60	1.07
50	1.12
40	1.14
30	1.17

## APPENDIX B

### Statistical Analysis of Data on Resistivity

In general the line of the plot of resistivity versus log % reduction will not pass exactly through any of the points as each point is subject to random error. Therefore each point is in error by an amount given by its deviation from the straight line. Therefore a statistical analysis by use of the least squares method was made of the plot of resistivity versus log % reduction. The general equation for this graph is of the form.

$$y = a + b \log x$$

or

$$y = a + bx'$$

Thus the error for the first point is given by:

$$e_1 = (a + bx'_1) - y_1$$

and so forth for each point. The sum of the square of the errors is an equation of the following form.

$$\sum(e^2) = (a + bx'_1 - y_1)^2 + (a + bx'_2 - y_2)^2 \text{ ----}$$

Then by differentiating with respect to "a" and "b" and setting these two equations equal to zero the minimum error is obtained. These are also the two normal equations. Simultaneous solution of the two normal equations yields the best solution of "a" and "b" which are then substituted into  $y = a + bx'$  or  $y = a + b \log x$  to obtain the equation of the line.



Rearranging the normal equations results in:

$$\sum y = \sum a + \sum b x$$

$$\sum xy = \sum ax + \sum b x^2$$

and these are used to determine the values of "a" and "b" in this analysis of the following data:

<u>% Reduction</u>	<u>Logx</u>	<u>y</u>
6	0.778	6.060
12	1.080	6.105
14	1.146	6.112
15	1.176	6.107
20	1.302	6.111
21	1.322	6.130
22.5	1.352	6.133
24	1.380	6.126
28.5	1.456	6.136
40	1.602	6.136

Solution of the first normal equation yields:

$$12.59 = 10a + 61.15b$$

and the solution of the second normal equation results in

$$77.08 = 61.19a + 374.25b$$

Then the result of simultaneous solution of the two equations yields values of "a" and "b" as follows:

$$a = 6.00$$

$$b = 0.009$$

and these result in the following equation:

$$y = 6.00 + 0.009 \log x$$

where: y = electrical resistivity

x = percent reduction

## VITA

Paul Fredric Becher was born February 13, 1941 in Buffalo, New York. His secondary education was obtained at Oak Ridge High School, Oak Ridge, Tennessee. He received his college education at the University of Missouri School of Mines and Metallurgy. In June, 1963, he was granted the Bachelor of Science Degree in Metallurgical Engineering.

In September, 1963, he returned to the Missouri School of Mines and Metallurgy to begin work on the Master of Science Degree in Metallurgical Engineering. He has pursued his graduate studies as a Ball Brothers Research Fellow.